Characterization of electron beams generated in a high-voltage pulse-line-driven pseudospark discharge

K. Ramaswamy, W. W. Destler, Z. Segalov, and J. Rodgers
Laboratory for Plasma Research, University of Maryland, College Park, Maryland 20742

Emittance and energy measurements have been performed on a high-brightness electron beam ($>10^{10}$ A/m^2 rad^2) with diameter in the range 1–3 mm and energy in the range 150–170 keV. This electron beam is generated by the mating of a hollow-cathode discharge device operating in the pseudospark regime to the output of a high-power pulse line accelerator. The measured effective emittance lies in the range between 30 and 90 mm mrad and increases with axial distance. Electron energy measurements indicate that the high-energy electrons are generated during the first 20–30 ns of the discharge. Both the emittance and energy experiments were performed at two different ambient argon gas pressures (92 and 152 mtorr). Beam expansion as a function of axial position has also been studied and a lower bound on the beam brightness has been obtained.

I. INTRODUCTION

The pseudospark discharge phenomenon was first reported by Christiansen and Schultheiss.[1] The pseudospark discharge is a gas discharge in a hollow cathode and a planar anode configuration operating on the low-pressure side of a characteristic breakdown curve which is similar to the Paschen curve for parallel electrodes. Highly pinched electron beams with high current densities (10^6 A/cm^2) have been observed to exit the discharge on-axis during the breakdown phase. Interest in these high-quality, high-current electron beams has been stimulated by their potential applications in such diverse areas as electron-beam lithography and plasma processing. In addition, the development of novel coherent radiation sources such as the free-electron laser and the stringent source requirements for advanced accelerators have spurred interest in new methods for producing low-emittance, high-brightness electron beams. Moreover, the high-power microwave tube community would welcome the development of high-brightness beam sources, especially if total beam current and energy could approach that currently achieved in high-power pulse-line accelerators.

Several experiments have been reported[2–4] over the last decade in which high-brightness electron beams have been produced in pseudospark devices operating in the voltage range 20–50 kV. Ion-focused electron beams with normalized brightness values as high as 10^{12} A/m^2 rad^2 have been produced. The extraction of these ion-focused electron beams into vacuum, however, is complicated by the low-energy and very high current density of these electron beams. The beams would quickly blow up if injected into vacuum due to the strong self-space-charge fields of the beam.

In order to reduce the self-space-charge fields, these beams should be generated at energies comparable to those achieved in the field-emission diodes associated with pulse line accelerators. With this objective in mind, we reported initial experiments[5] wherein a high-power pulse-line accelerator was mated to a hollow cathode discharge experiment operating in the pseudospark regime. In this article we report experiments undertaken to characterize the beam emittance and energy. This article is organized as follows. The experimental setup is described in Sec. II and energy studies are described in Sec. III. Emittance studies are discussed in Sec. IV and conclusions and future experiments are discussed in Sec. V.

II. EXPERIMENTAL CONFIGURATION

The experimental configuration is shown in Fig. 1. A multigap hollow cathode discharge device is mated in series with a 200 Ω resistor to the output of a pulse line accelerator which is capable of routine operation at 150–600 kV, 5–40 kA, 1 μs. This pulse-line accelerator, which normally operates at 200–800 kV, 40–120 kA, 100 ns, was modified to produce a longer pulse duration by eliminating the output pulse forming switch and connecting the load directly to the output of the pulse transformer via a water coax section. The experimental configuration used for the present studies is different from the setup described in our last experiment[5] in two ways.

In the studies reported previously, a matching resistor of 10 Ω was used. This was changed to a current limiting resistor of 200 Ω for the following reasons. The peak line current in our earlier setup was about 20 kA and the extracted beam current rose to about 3 kA after voltage collapse. The peak ejected electron-beam current was therefore a small fraction of the observed line current, an indication that most of the postcollapse current flows from electrode to electrode and is returned to ground at the anode. Most of the high-energy electrons are emitted in a short burst of approximately 20 ns before collapse. In an attempt to delay the switch collapse to the highly emissive final conduction state, it was decided to limit the line current in the system.

In addition, the number of grading electrodes was reduced from ten to six. This was done to increase the electric field between the anode and cathode and allow more reliable discharge formation. Each electrode plate had an on-axis aperture 0.63 cm in diameter. The electrons generated in the

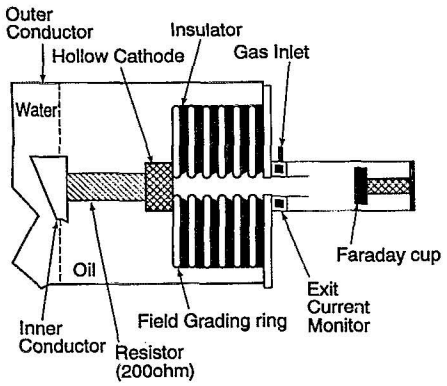

FIG. 1. Basic experimental configuration.

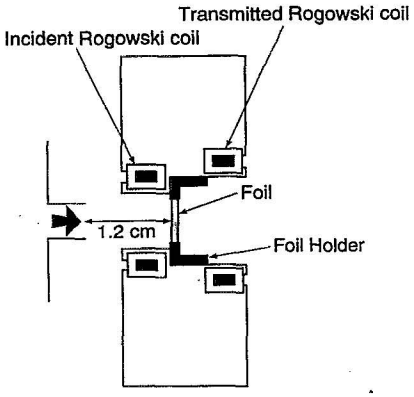

FIG. 3. Schematic of range-energy probe.

hollow cathode region were accelerated through these apertures to the extraction point on the anode side of the device. The discharge was initiated in argon gas with ambient pressures in the range of 92–150 mTorr.

A. Diagnostics

The exit beam current monitor used is a fast current transformer that measures the total electron current ejected out the downstream end of the device. A Faraday cup was also used to measure the total beam current as a function of distance along the system axis. A capacitive probe was used to measure the line voltage and a B-dot probe was used to measure the line current in the pulse line accelerator. In addition, special diagnostics were constructed to study electron-beam energy and emittance. These are described in later sections. A Pirani gauge was used to measure the ambient gas pressure in all experiments.

Typical pulse-line voltage (upstream) and current wave forms (exit current monitor) are shown in Fig. 2. The voltage is seen to rise smoothly to about 170 kV prior to voltage collapse. Note that the voltage does not immediately fall to zero as in our previous experiment[5] because of the presence of the current limiting resistor. In these experiments, the charging voltage was approximately 170 kV. The exit current monitor records a peak injected electron beam current of about 1 kA. If the capacitances in the system are ignored and the current is assumed to be determined by the current limiting resistor, a current of about 850 A would be expected at this operating voltage. The fact that a peak ejected current greater than 850 A is observed suggests that the various capacitances in the system (multielectrode pseudospark stack, line capacitance) store charges as the line is charged and quickly discharge when the voltage collapses, contributing to the ejected current. This is a preliminary hypothesis which will be investigated in future experiments.

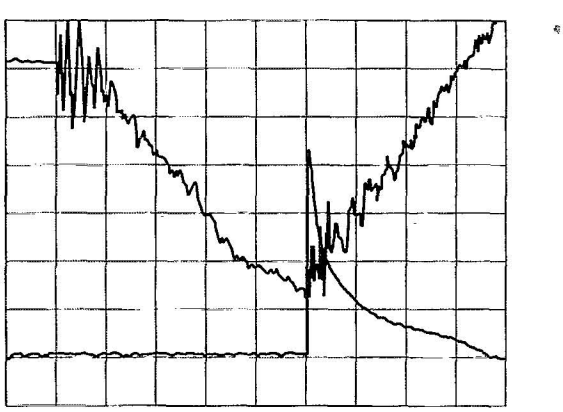

FIG. 2. Typical pulse line voltage (top, 37 kV/div) and exit beam current (bottom, 0.5 kA/div) wave forms. Both wave forms are 500 ns/division.

III. ENERGY STUDIES

In order to determine the beam energy, electron range-energy studies were undertaken. For these studies a range-energy probe was made with Rogowski coils on both sides to measure the incident and transmitted current simultaneously, as shown in Fig. 3. Figure 4 shows current wave forms of the incident and transmitted beam pulse without any stopping foil. As is evident, the wave forms are in good agreement. Energy-range studies were performed with aluminum foils ranging in thickness from 0.35 mil (0.008 mm) to 3 mils (0.0762 mm) and also with Mylar varying in thickness between 1 mil (0.0254 mm) and 7 mil (0.18 mm). Figure 5(a) shows the incident and transmitted current for 1 mil Mylar, and Fig. 5(b) shows the incident and transmitted current for 0.5 mil aluminum. These studies were conducted at two ambient argon gas pressures of 92 and 152 mTorr and the breakdown voltage ranged from 162 to 172.3 kV. In the case of

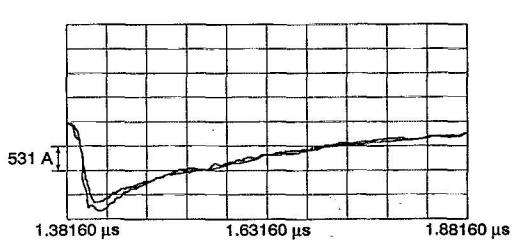

FIG. 4. Incident and transmitted electron beam current vs time without any stopping foils.

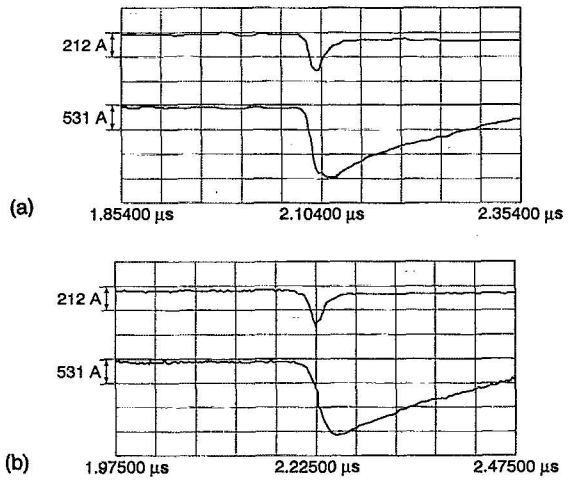

FIG. 5. (a) Incident and transmitted electron beam current vs time for a 1 mil (0.0254 mm) Mylar stopping foil (breakdown voltage 162–172.3 kV, ambient gas pressure 92 mTorr). (b) Incident and transmitted electron beam current vs time for a 0.5 mil (0.0127 mm) aluminum stopping foil (breakdown voltage 162–172.3 kV, ambient gas pressure 92 mTorr).

Mylar (see Fig. 6), there is a clear difference in the results obtained at the two pressures. This is also observed in the aluminum foil (Fig. 7), although the difference is not as great. One reason for this difference in transmission between the two ambient pressures could be that the lower-energy electrons lose energy via scattering with the ambient gas molecules. Figure 8 shows the mean-free-path lengths for electron-impact ionization collisions with argon gas at two different pressures (92 and 152 mTorr).[6] Note that for the high-energy electrons collisions with the ambient gas molecules are not an issue (mean free path ~1.8 m).

In order to estimate the spread in energy in the electron beam, a set of theoretical energy-range curves for monoenergetic electron beams was created based on the formula derived by Bleuler and Zunti.[7] The transmission defined as the fraction N/N_0 of the initial intensity remaining in a homogeneous beam of electrons (initial energy E_0) after traversing a distance x through an absorber is

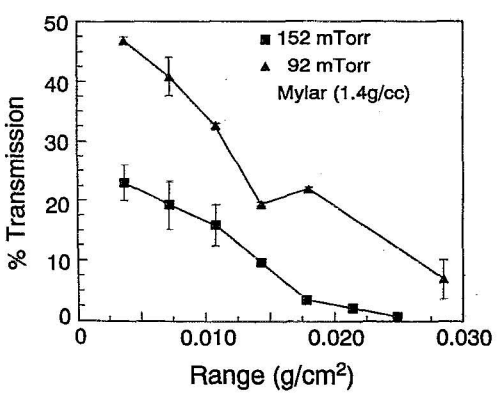

FIG. 6. Percentage transmission vs range in mylar at 92 and 152 mTorr ambient gas pressure at charging voltages in the range 162–172.3 kV.

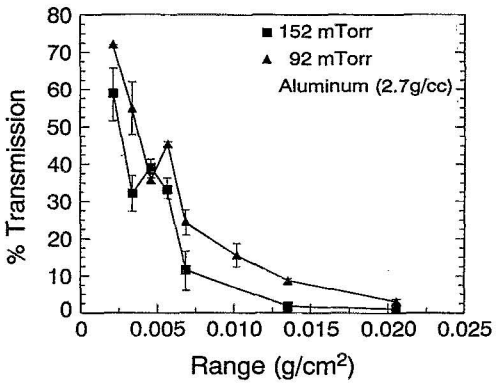

FIG. 7. Percentage transmission vs range in aluminum at 92 and 152 mTorr ambient gas pressure at charging voltages in the range 162–172.3 kV.

$$\frac{N}{N_0} = \exp\left(-\int_0^x \alpha(x)dx\right), \tag{1}$$

where

$$\alpha(x) = 14.2\left(\frac{E+0.511}{E(E+1.022)}\right)^2 \text{ cm}^{-1}. \tag{2}$$

Here E is the energy in MeV of the electrons after passing through a thickness x. Bleuler and Zunti assume that for a given E_0, E and x may be related through a range-energy curve. These curves were verified against the experimental data of Marshall and Ward.[8] The practical ranges of the theoretical curves are about 14% less than those of the experimental curves. Figure 9 shows the data from the experiment (aluminum) superimposed on the theoretical curves for monoenergetic electrons.

From the results the following conclusions may be drawn. First, the electron beam clearly has a significant time integrated spread in energy. Second, the high-energy electrons constitute a small fraction of the beam. The second conclusion is also evident from Fig. 5 where the high-energy

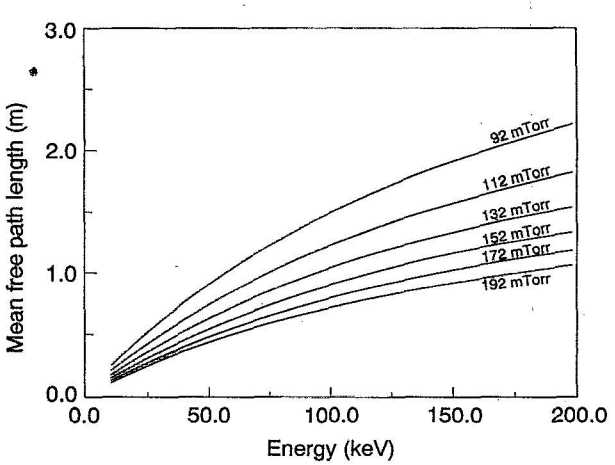

FIG. 8. Mean free path between electron-argon gas molecule impact ionizing collisions at different ambient gas pressures vs energy.

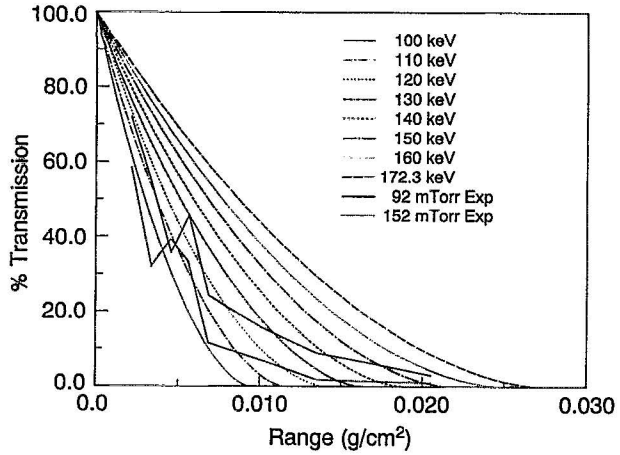

FIG. 9. Theoretical range-energy curves for monoenergetic electrons in aluminum. The experimental curves (breakdown voltage in the range 162–172.3 kV) at two different ambient gas pressures (92 and 152 mTorr) are superimposed.

electrons are observed to be produced in the first 20 ns and at lower current levels than are the lower-energy electrons.

IV. EMITTANCE MEASUREMENTS

The effective emittance,[9] which is widely used as a measure of beam quality, is defined as

$$\epsilon = 4(\langle X^2\rangle\langle X'^2\rangle - \langle XX'\rangle^2)^{0.5}, \tag{3}$$

where X' is the gradient of the particle trajectory given by $X' = dX/dz = p_X/p_z$, and the angular brackets denote average values over the two-dimensional trace space as

$$\langle\phi\rangle = \int \phi\rho(X,X')dX\,dX', \tag{4}$$

where ρ is the projected density in two-dimensional trace space and is assumed to be normalized.

The emittance is measured using the slit-hole method.[10] The experimental setup is shown in Fig. 10. The electron beam passes through the slit mask and forms four to seven beamlets which then strike a radiochromic film which acts as a beam detector. The detector is located 13 mm from the slit mask. The slit mask was made by carefully laying 10 mil (0.254 mm) wires on two 56 threads/in. screws. The slit mask is shown in Fig. 11. In order obtain clear images and

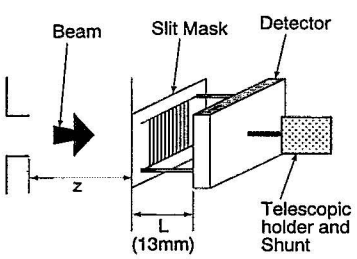

FIG. 10. Experimental configuration for emittance measurement.

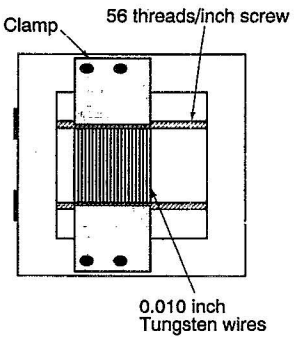

FIG. 11. Slit mask for emittance measurement.

also to determine the emittance of only the high-energy electrons, a 5 mil (0.127 mm) Mylar film is used as a protective cover for the radiochromic film. The Mylar film acts as a filter eliminating electrons of energy less than 100 keV. The response of this film is linear with electron exposure.[11] The exposed film is later scanned to obtain a distribution in the image plane. Figure 12 shows a microdensitometer scan of a typical shot. The emittance was measured both as a function of axial distance as well as ambient gas pressure. Figure 13 shows the effective emittance as a function of gas pressure as well as axial distance. The voltage on the pulse-line accelerator varied shot to shot from 148 to 172.3 kV. Hence, the invariant normalized emittance $\epsilon_n = \beta\gamma\epsilon$ was also calculated (see Fig. 14). From Figs. 13 and 14, it is evident that the emittance grows as the axial distance is increased. The emittance of the electron beam lies between 30 and 90 mm mrad. Space-charge forces are a likely reason for the observed growth in beam emittance with axial distance. This will be investigated in future experiments.

The plot of beam radius versus axial position was obtained for two different gas pressures and is shown in Fig. 15. The beam radius was determined by scanning the image of the electron beam on radiochromic film. Based on the beam current measured after transmission through a 5 mil Mylar film (100 A), a lower bound on the normalized brightness has been derived. The normalized brightness is defined as

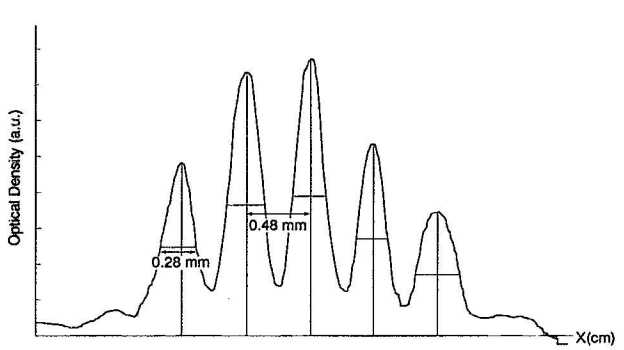

FIG. 12. Microdensitometer scan showing optical density of images vs transverse position.

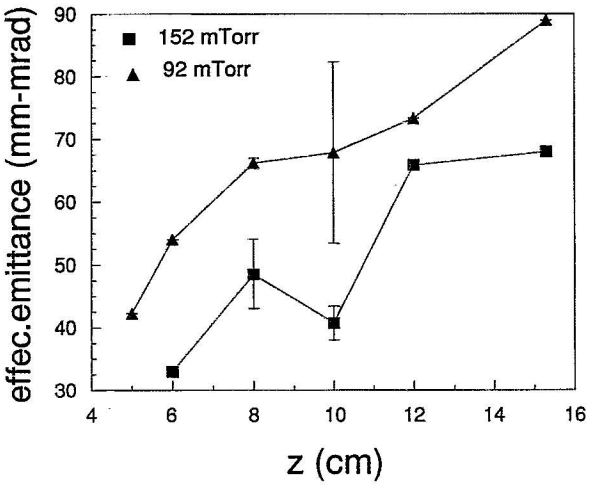

FIG. 13. Effective emittance vs axial position at different ambient gas pressures (92 and 152 mTorr).

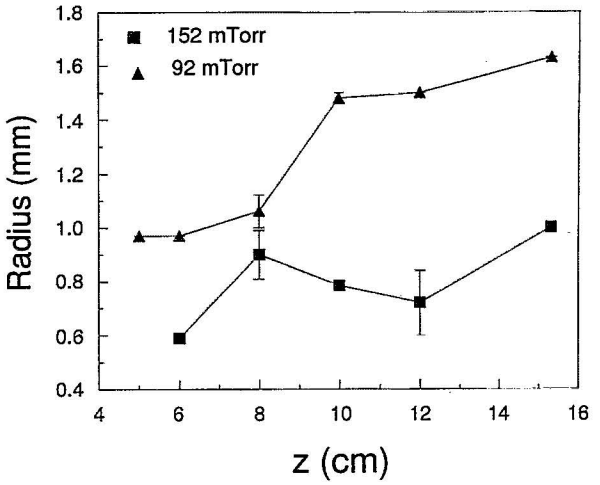

FIG. 15. Electron beam radius vs axial position at different ambient gas pressures (92 and 152 mTorr).

$$B_n = \frac{2I}{\pi^2 \epsilon_n^2}, \tag{5}$$

where ϵ_n is the normalized emittance. Figure 16 shows the beam brightness at various axial distances at two different ambient gas pressures.

V. CONCLUSIONS AND FUTURE EXPERIMENTS

In this article experiments designed to characterize the high-brightness electron beams generated in a high-voltage pulse-line-driven pseudospark discharge are reported. The major conclusions to be drawn from this work are as follows.

(1) High-brightness ($>10^{10}$ A/m^2 rad^2) electron beams have been generated in a hollow cathode discharge operating at approximately 170 kV. Ejected electron-beam diameters in the range of 1–3 mm have been observed.

(2) The high-energy component of the electron beam has an energy comparable to the discharge voltage (170 keV) and is generated in a 20–30 ns burst immediately before voltage collapse.

(3) The effective emittance of the ejected high-energy component of the electron beam was measured and found to be in the range 30–90 mm mrad, a value comparable to photocathode beam sources constructed at considerably greater cost and complexity.

(4) Beam emittance and brightness deteriorate as the beam propagates away from the output of the device, probably due to space-charge forces.

Future experiments are planned in which the discharge voltage will be increased to 400 kV to determine if the high-brightness and low-emittance values observed in these experiments are scalable to higher beam energies. In addition, injection of the beam into vacuum will be studied at these higher electron energies to determine whether such beams can actually be injected into rf structures, FELs, etc.

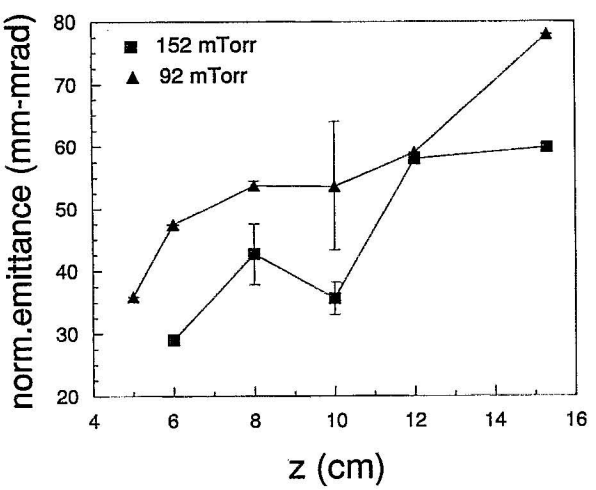

FIG. 14. Normalized emittance vs axial position at different ambient gas pressures (92 and 152 mTorr).

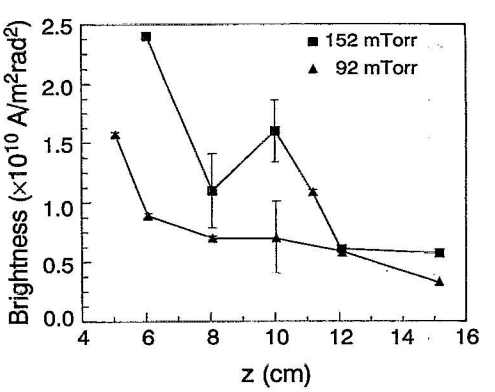

FIG. 16. Beam brightness (lower bound) vs axial position at different ambient gas pressures (92 and 152 mTorr).

ACKNOWLEDGMENTS

We would like to acknowledge useful discussions with Professor M. J. Rhee and Chengjun Liu. It is also a pleasure to acknowledge the technical support of Jay Pyle and Doug Cohen. This project was supported by the U.S. Department of Energy.

[1] J. Christiansen and Ch. Schultheiss, Z. Phys. A **2990**, 35 (1979).
[2] K. K. Jain, E. Boggasch, M. Reiser, and M. J. Rhee, Phys. Fluids B **2**, 2487 (1990).
[3] W. Benker, J. Christiansen, K. Frank, H. Gundel, W. Hartman, T. Redel, and M. Stelter, IEEE Trans. Plasma Sci. **PS-17**, 754 (1989).
[4] P. Choi, H. H. Chuaqui, M. Favre, and E. S. Wyndham, IEEE Trans. Plasma Sci. **PS-15**, 248 (1987).
[5] W. W. Destler, Z. Segalov, J. Rodgers, K. Ramaswamy, and M. Reiser, Appl. Phys. Lett. **62**, 1739 (1993).
[6] M. Reiser, *Theory and Design of Charged Particle Beams* (Wiley, New York, in press).
[7] E. Bleuler and W. Zunti, Helv. Phys. Acta **19**, 375 (1946).
[8] J. Marshall and A. G. Ward, Can. J. Research. A **15**, 39 (1937).
[9] P. M. Lapostolle, IEEE Trans. Nucl. Sci. **NS-18**, 1101 (1971).
[10] M. J. Rhee and R. F. Schneider, Particle Accelerators **20**, 133 (1986).
[11] W. L. McLaughlin, R. M. Uribe, and A. Miller, Radiat. Phys. Chem. **22**, 333 (1983).